

# Object Instance Retrieval in Assistive Robotics: Leveraging Fine-Tuned SimSiam with Multi-View Images Based on 3D Semantic Map

Taichi Sakaguchi<sup>1</sup>, Akira Taniguchi<sup>1,\*</sup>, Yoshinobu Hagiwara<sup>1</sup>, Lotfi El Hafi<sup>1</sup>,  
Shoichi Hasegawa<sup>1</sup>, and Tadahiro Taniguchi<sup>1</sup>

**Abstract**—Robots that assist in daily life are required to locate specific instances of objects that match the user’s desired object in the environment. This task is known as Instance-Specific Image Goal Navigation (InstanceImageNav), which requires a model capable of distinguishing between different instances within the same class. One significant challenge in robotics is that when a robot observes the same object from various 3D viewpoints, its appearance may differ greatly, making it difficult to recognize and locate the object accurately. In this study, we introduce a method, SimView, that leverages multi-view images based on a 3D semantic map of the environment and self-supervised learning by SimSiam to train an instance identification model on-site. The effectiveness of our approach is validated using a photorealistic simulator, Habitat Matterport 3D, created by scanning real home environments. Our results demonstrate a 1.7-fold improvement in task accuracy compared to CLIP, which is pre-trained multimodal contrastive learning for object search. This improvement highlights the benefits of our proposed fine-tuning method in enhancing the performance of assistive robots in InstanceImageNav tasks. The project website is <https://emergentsystemlabstudent.github.io/MultiViewRetrieve/>.

## I. INTRODUCTION

In indoor environments, when the user does not know the location of the desired object, a robot’s ability to discover an object identical to a query image previously captured by the user becomes important. For example, if a user wants the robot to check whether their cell phone is on the chair, the robot needs to move close to the table. However, multiple “chairs” exist in the environment, as shown in Fig. 1. To efficiently execute tasks in such situations, it is necessary to distinguish between the instances of the same class of objects present in the environment, identifying those desired by the user and those that are not relevant. **Instance Specific Image Goal Navigation (InstanceImageNav)** was proposed as a task for locating a specific instance to the query image within the environment [1]. When a robot observes an object while exploring in a 3D space, images of the same instance could include images from various 3D viewpoints, such as observing it from the back side, as shown in Fig. 1 (top). In

This work was supported by JSPS KAKENHI Grants-in-Aid for Scientific Research (Grant Numbers JP23K16975, 22K12212) and JST Moonshot Research & Development Program (Grant Number JPMJMS2011).

<sup>1</sup>Taichi Sakaguchi, Akira Taniguchi, Yoshinobu Hagiwara, Lotfi El Hafi, Shoichi Hasegawa, and Tadahiro Taniguchi are with Ritsumeikan University; 1-1-1 Noji-Higashi, Kusatsu, Shiga 525-8577, Japan. {sakaguchi.taichi, a.taniguchi, yhagiwara, lotfi.elhafi, hasegawa.shoichi, taniguchi}@em.ci.ritsumeikan.ac.jp

\*Corresponding author.

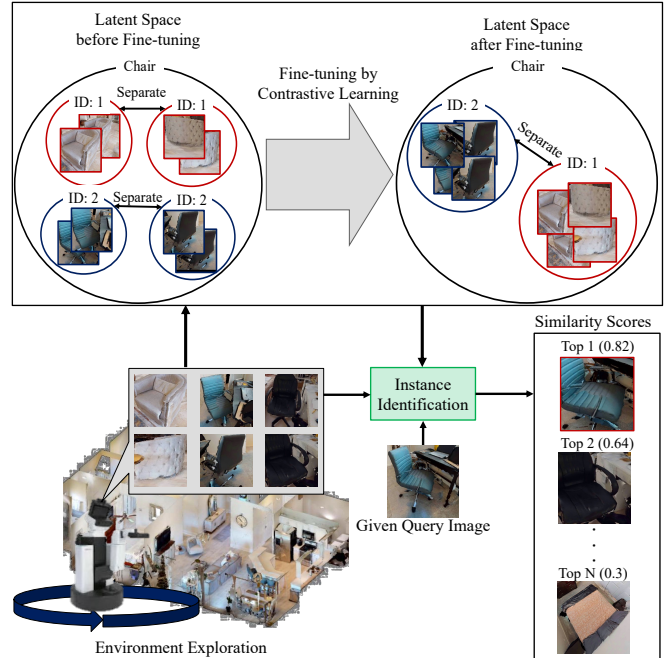


Fig. 1. Tasks and challenges addressed by this study. The robot observes the same object from various angles of view. Therefore, a model that learns the similarities between images from different 3D viewpoints is required to identify objects that are the same as a given query image.

this case, it could be difficult to recognize them as the same instance. Thus, a challenge will be calculating the similarity of images of the same object from different 3D viewpoints.

Contrastive language-image pre-training (CLIP) [2] is gaining attention for its application in various robotics tasks, such as NLMaP and CLIP-Fields [3], [4]. CLIP pre-trains via multimodal contrastive learning with pairs of images and their captions. CLIP models effectively group objects with the same name into categories, resulting in excellent performance on category-based tasks. However, this approach can harm instance-based fine-grained tasks such as InstanceImageNav (see Section II-A). Therefore, we have a key insight using unimodal contrastive learning with image pairs to address this issue and improve instance-based performance.

This study explores methods that pre-train via contrastive learning with image pairs [5]–[8] (see Section III-A for details). In particular, self-distillation methods, such as SimSiam [6] and DINOv2 [7], involve learning to make feature vectors of images, generated through data augmentation from a single image, similar. This approach aims to achieve higher

similarity in feature vectors for images of the same instance, making it effective for tasks requiring instance identification. Models trained by unimodal contrastive learning between images are suggested to acquire discriminative representations between instances [7]. Therefore, we consider the feature vector obtained from an image encoder learned through contrastive learning to be more effective than that obtained from the CLIP’s image encoder for solving the InstanceImageNav task. The proposed system records instance feature vectors learned by contrastive learning and their position in the map. We verify that self-distillation has a higher success rate than CLIP’s image encoder in the InstanceImageNav task.

An important approach in this study is to fine-tune the latent space so that the feature vectors of multi-view images of the same instance become closer (see Fig. 1 (top) and Section II-B). Robots can explore independently, collect data sets of their environment, and learn. In this study, the proposed system automatically labels images using the robot’s 3D semantic map. This approach will improve the similarity between multi-view images of the same object, allowing for simultaneous performing contrastive learning and image label classification within a self-supervised learning framework. Such an approach has the potential to be applied not only to home environments but also to image searches for products in convenience stores and warehouses.

The aims of this study are shown in follows. (i) Investigate the image encoder trained with contrastive learning [5]–[7] is more suitable for instanceImageNav than CLIP models trained with multimodal contrastive learning. (ii) Investigate that self-supervised learning with observed object images with pseudo-labels based on 3D semantic maps can acquire instance-specific multi-view representations.

The main contributions of this study are as follows:

- 1) We show that models from contrastive learning between images are superior to CLIP, which is multimodal contrastive learning between vision and language, for instance-level object identification.
- 2) We show that increasing the similarity between identical object images from different viewpoints observed by the robot in the framework of self-supervised learning improves object instance retrieval that is identical to the query image.

## II. PROBLEM STATEMENT

This study tackles two critical challenges essential for advancing the InstanceImageNav using contrastive learning.

### A. Problem 1: Zero-shot InstanceImageNav by Contrastive Learning

CLIP solves zero-shot classification tasks with high accuracy using the similarities between object class name and image feature vectors [2]. However, it has been suggested that CLIP is unsuitable for fine-grained tasks [9]–[11] that require something from sub-classes within the same class. Hence, we hypothesize that using an encoder trained through self-distillation for the InstanceImageNav task is more effective than CLIP’s image encoder.

### B. Problem 2: Visual Feature Similarity in Multi-View Images

When a robot explores the environment and observes an object, it observes the object from various 3D viewpoints. In this case, the problem arises that the success rate of InstanceImageNav decreases due to the possibility that the appearance may be significantly different. In addition, it is difficult to maximize the similarity between images using contrastive learning with such a dataset of multi-view images, as shown in Fig. 1 (top left). Generally, contrastive learning uses data augmentation to maximize the similarity between two different images in which a two-dimensional viewpoint change is performed on a single image. To improve instance identification from different viewpoints, it’s crucial to fine-tune a pre-trained model on multi-view images of the same instance collected by the robot, enhancing the similarity between these images.

## III. RELATED WORK

This section summarizes related work on the two aspects of contrastive learning and object retrieval.

### A. Contrastive Learning

Contrastive learning is a type of method for learning image feature representation in a self-supervised manner. Contrastive learning methods are broadly divided into methods that use negative pairs [5], [8] and methods called self-distillation that do not use negative pairs [6], [7], [12], [13]. Methods using negative pairs train by data augmentation to maximize the similarity between the same images and minimize the similarity between different images. Since training is conducted to maximize the similarity between images of the same instances, it is thought that a model that has learned image feature representation through contrastive learning is learning discriminative representation between different instances [14]. Therefore, models pre-trained by contrastive learning are suitable for tasks requiring discrimination between instances, such as InstanceImageNav [1].

As a self-distillation method, SimSiam has proposed a method where two different images generated from a single image through data augmentation are input into a CNN, aiming to maximize the cosine similarity of their feature vectors [6]. Furthermore, DINOv2 inputs images generated through data augmentation into separate Vision Transformers (ViTs), aiming to minimize the cross-entropy between the class tokens and the patch tokens of the two ViTs, respectively [7]. Additionally, Oquab *et al.* experimentally demonstrated that their self-distillation method achieved high accuracy in similar image retrieval from a database for images of objects identical to those in the query image [7].

### B. Object Retrieval

To solve InstanceImageNav, Kranz *et al.* proposed a method in which navigation policies are learned through deep reinforcement learning, and the robot does not have an explicit environment map [1]. However, this approach requires a large amount of data and suffers from over-fitting.

In addition to methods for solving object search tasks based on deep reinforcement learning or imitation learning [1], [15], methods that utilize an explicit environment map of the robot were also proposed [3], [4]. For example, Chen *et al.* proposed a method to calculate the feature vector of an observed object image using CLIP’s image encoder and construct a semantic map called NLMap that records the position information of the object feature vector [3]. Specifically, an instruction such as “Bring me a snack” is given, the word feature vector of the target object “snack” is calculated using CLIP’s text encoder, and the word feature vector and the word feature vector are calculated. The object search task is solved by calculating the similarity between the object feature vectors recorded in NLMap and the word feature vector and identifying the position of the most similar object. A method in which a robot uses an explicit map of the environment for object search tasks was shown to have a higher success rate in real-world tasks than a method in which a robot learns a navigation policy in an end-to-end manner. [16]. Therefore, this study adopts an approach with the explicit environment map, inspired by NLMap [3].

In addition, CLIP-Fields constructs a 3D semantic map by learning so that the feature vectors of each point on the 3D point cloud map are similar to the feature vectors obtained from CLIP’s image encoder [4]. CLIP-Fields solved the object search task by calculating the similarity between the feature vector obtained from CLIP’s text encoder and the feature vector of the point cloud of the 3D semantic map and searching for the target object’s position.

Semantic map methods using CLIP feature vectors, such as NLMap [3] and CLIP-Fields [4], can perform zero-shot object search tasks since CLIP has high accuracy for zero-shot classification tasks. However, as explained in Section III-A, CLIP is not good at the task of fine-grained classification task. Therefore, the semantic map created using CLIP feature vectors is unsuitable for InstanceImageNav’s task. In addition, Shafiqullah *et al.* suggests that it is possible to coarsely identify the location where a given image query was taken using CLIP-Fields. However, whether it is possible to search for the location of a specific object as required by InstanceImageNav has not been verified.

#### IV. PROPOSED SYSTEM

In the proposed system, a robot explores the environment, identifies the instance identical to a given query image from among the collected object images, and uses a 3D semantic map of the environment to locate the target object’s position. In addition, we propose a method, **Semantic Instance Multi-view Contrastive Fine-tuning (SimView)**, for fine-tuning pre-trained models using a self-supervised learning framework to improve task accuracy in the environment. Fig. 2 shows the diagram of our proposed system.

##### A. Vector Registration by Registration Module

1) *Exploration of Environment:* We set up exploration points at the same intervals in the free space on a 2D map, and the robot explores the environment by visiting these

exploration points. This study consistently places exploration points at 30 [cm] intervals.

2) *Observation of Object Image:* While the robot explores the environment, as illustrated in Fig. 2, 2D mask images are generated using ray-tracing with the segmented 3D map and camera pose. Generating mask images from the 3D map allows the same object to be associated across different frames. The observed mask images are converted into Bounding Boxes (BBoxes), and the robot extracts the BBoxes regions from the observed RGB images to observe the objects. When extracting the BBoxes of each object from the RGB image, it is adjusted to match the longer side of the BBox. In addition, areas outside the original RGB image are interpolated with only black.

3) *Registration of Feature Vector of Object Image:* The images of observed objects are pre-processed and fed into a pre-trained encoder to convert them into feature vectors. In this study, observed images are resized to  $256 \times 256$ ; then, a  $224 \times 224$  pixel image is cropped around the image’s center and normalized before inputting into the encoder. The types of transformations used for pre-processing and the parameters used for normalization follow those used in previous studies [6]. Additionally, when the same object is observed multiple times in the environment, the observed feature vectors for each object are recorded as a single set.

##### B. Self-Supervised Fine-Tuning with Instance Classifier

This module fine-tuned the image encoder, which was pre-trained by contrastive learning using self-supervised learning, object images observed by the robot while exploring the environment, and their pseudo-labels. When a robot explores the environment and observes objects, images of the same instance include images observed from various angles of view. In a preliminary experiment, we confirmed that when fine-tuning a pre-trained model using only contrastive learning on such a dataset, the accuracy of discrimination between instances is worse than that of the trained model. Therefore, we propose a method to train a linear classifier simultaneously with contrastive learning. We use object instance ID  $y_{true}$  obtained from a 3D semantic map of the robot’s environment as pseudo labels.

In addition, the contrastive learning method using negative pairs is recommended to be trained with a very large batch size and requires a large amount of data for learning [5]. Then, to conduct fine-tuning, it is necessary to continue exploring the environment for a long time and collecting images of objects. Therefore, we use SimSiam for fine-tuning, which allows learning even with a small batch size [6]. This module conducts fine-tuning to minimize the following loss function:

$$\mathcal{L} = \frac{1}{2} \{ \text{CosSim}(h, z') + \text{CosSim}(h', z) \} + \frac{1}{2} \{ \text{CE}(y_{pred}, y_{true}) + \text{CE}(y'_{pred}, y'_{true}) \}, \quad (1)$$

where  $\text{CE}()$  and  $\text{CosSim}()$  denote cross-entropy and cosine similarity.  $z$  and  $h$  are the outputs of SimSiam’s projector and predictor of the object image  $x$  observed by the robot.  $y_{pred}$

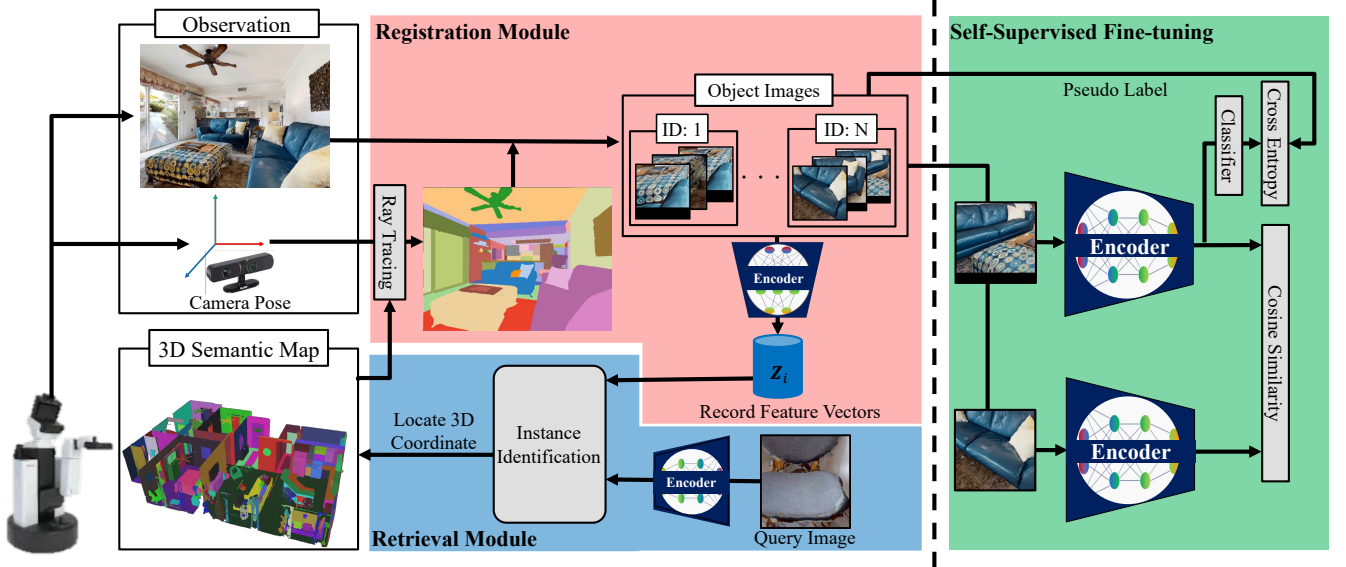


Fig. 2. Overview diagram of the proposed method. The red area indicates the recording of feature vectors for each object, while the blue area indicates performing a similar object search.

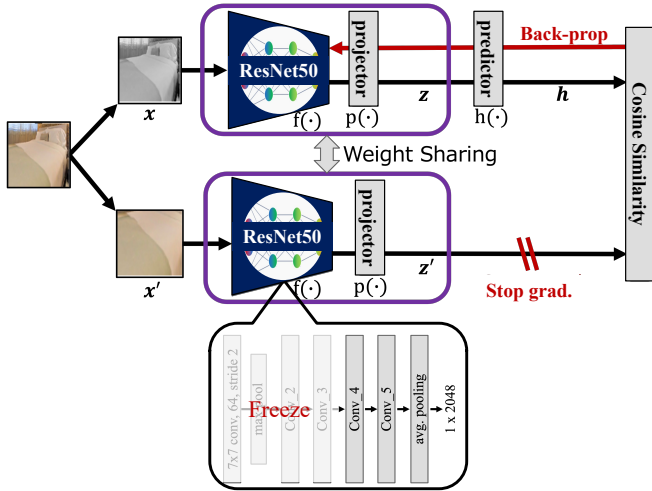


Fig. 3. Parameters to be fixed during fine-tuning. Fix all parameters up to the third block of ResNet50 used in SimSiam

is the instance ID of  $x$  predicted by classifier. Here,  $x$  and  $x'$  are different images of the same instance generated by data augmentation. The same goes for other primed variables,  $z'$ ,  $h'$ ,  $y'_{pred}$ , and  $y'_{true}$ .

In addition, it is possible to quickly introduce the robot into the task environment based on reducing the time required for fine-tuning. Therefore, we use a method to reduce the time required for fine-tuning by fixing some parameters during fine-tuning. Fig. 3 shows the relevant parts of the parameters fixed during fine-tuning. Specifically, the parameters up to the third block of ResNet50 [17] used in SimSiam are fixed, and the other parameters are fine-tuned.

Please refer to the Appendix for details on the effectiveness of training SimSiam with a classifier.

### C. Instance Identification by Retrieval Module

The given query image  $I_q$  is input into a pre-trained encoder, resulting in a feature vector denoted as  $q$ . Furthermore, we represent the observed feature vectors with instance ID  $i$  as a set  $Z_i = \{z_{i,n}\}_{n=1}^{N_i}$ .  $N_i$  denotes the number of times the object with instance ID  $i$  was observed.

The cosine similarity between the query image  $q$  and observed feature vectors  $Z_i$  is calculated as  $\text{CosSim}(z_{i,n}, q) = \frac{z_{i,n} \cdot q}{\|z_{i,n}\| \|q\|}$  for each set of feature vectors corresponding to each instance ID, as follows:

$$m_i = \max(\{\text{CosSim}(z_{i,n}, q)\}_{n=1}^{N_i}). \quad (2)$$

From multiple similarities, the maximum value  $m_i$  is selected. Since it is known that an image encoder trained by contrastive learning embeds the image on the surface of a spherical space [18].

Finally, the instance ID  $J_{\text{target}}$  with the highest similarity among the set of maximum similarities  $\{m_j\}_{j=1}^J$  for each instance is obtained, as follows:

$$J_{\text{target}} = \underset{j}{\text{argmax}}(\{m_j\}_{j=1}^J). \quad (3)$$

The target object's position is obtained using the instance ID  $J_{\text{target}}$  from the search results and the 3D semantic map. The robot could navigate to the target position using the map.

## V. EXPERIMENT

This experiment aims to verify that an image encoder pre-trained by contrastive learning only image pairs is more suitable for identifying the same object as the query image than CLIP and to verify the effectiveness of fine-tuning using images observed by the robot.

TABLE I  
RESULTS OF AVERAGING MAP IN EACH ENVIRONMENT FROM 10 REPEATED TRIALS OF SIMILAR IMAGE SEARCH

Comparison Methods	Arch.	Env. 1	Env. 2	Env. 3	Env. 4	Env. 5	Env. 6	Env. 7	Env. 8	Env. 9	Avg.
SimView (Ours)	ResNet50	<b>0.79</b>	<b>0.67</b>	<b>0.68</b>	<b>0.91</b>	<b>0.68</b>	<b>0.45</b>	<b>0.72</b>	<b>0.74</b>	<b>0.8</b>	<b>0.72</b>
SimSiam [6]	ResNet50	<b>0.70</b>	0.58	0.56	0.80	0.65	0.41	0.63	0.68	0.75	0.64
DINOv2 [7]	ViT-B/14	0.51	0.48	0.45	0.66	<b>0.71</b>	0.41	0.55	0.44	0.61	0.54
SimCLR [5]	ResNet50	0.65	0.56	0.52	<b>0.83</b>	0.64	<b>0.45</b>	0.66	0.62	0.75	0.63
✓CLIP [2]	ResNet50	0.51	0.36	0.35	0.51	0.48	0.44	0.42	0.44	0.59	0.46
✓CLIP [2]	ViT-B/16	0.56	0.38	0.37	0.47	0.48	0.37	0.38	0.35	0.48	0.43

The methods marked with ✓ represent those pre-trained through contrastive learning between text and images.

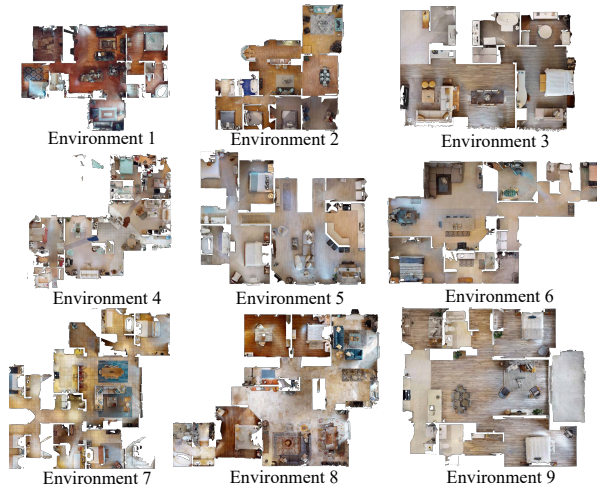


Fig. 4. Allocated view of the nine environments used in the experiment

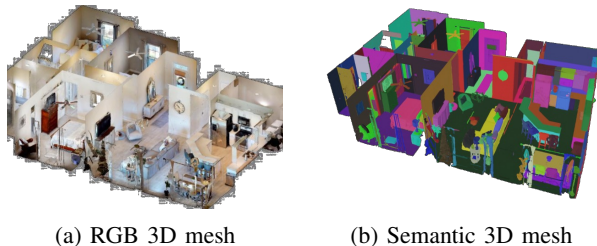


Fig. 5. Example 3D mesh data which is included in HM3D.

### A. Dataset

We utilize nine 3D meshes from Habitat Matterport 3D (HM3D) created by scanning real home environments [19]. These nine 3D meshes are scans of single-floor domestic environments, as shown in Fig. 4. As shown in Fig. 5, HM3D includes 3D meshes containing RGB data and 3D meshes segmented by each instance. In this experiment, we use the 3D meshes containing RGB data with the habitat simulator [20] as a simulation environment, while we employ the segmented 3D meshes as the 3D semantic map of the environment that the robot has.

Furthermore, we used images included in the dataset proposed by Krantz *et al.* [1] as query images. This dataset includes parameters such as the camera’s position, orientation, and resolution when capturing a particular instance. Based on this information, images were captured, and using

a method similar to the one described in Section IV-A.2, only the regions of interest for the target instances were cropped to collect the query images.

In addition, this dataset contains query images for over ten different instances for each environment, all of which belong to one of the six classes: “bed,” “chair,” “TV,” “plant,” “toilet,” or “couch.”

### B. Experiment Settings

Stochastic Gradient Descent (SGD) was used as the optimizer for all conditions. In the training process, we unified several hyperparameters across different training conditions. The batch size was set to 32, with a learning rate of 0.07. We used a weight decay of  $1.5 \times 10^{-6}$  and a momentum of 0.9. The training was conducted for a total of 100 epochs. These hyperparameters were chosen to ensure consistency and comparability in our experiments. The learning rate was allowed to decay as the training progressed using Cosine Scheduler [21]. Four types of data expansion were used during training: crop and resize, color jitters, grayscale, and horizontal flip. We use a PC with Intel Core i9-9900K and an Nvidia RTX 2080 in this experiment.

### C. Metrics

We use the mean Average Precision (mAP), used in similar image retrieval benchmark [22], for evaluation metrics. mAP is computed by averaging the Average Precision (AP) for each instance. AP is calculated as  $AP = \frac{1}{N} \sum_{n=1}^N P_n$  where  $N$  is the number of instances and  $P_n$  is precision. Since the number of images to be retrieved is one,  $P_n$  is 1 if the retrieved image is the same instance as the query image and 0 otherwise. Then, mAP is calculated as the average AP when  $K$  different query images are prepared for each instance. Therefore, the calculation of mAP is shown as follows:

$$AP = \frac{1}{K} \sum_{k=1}^K AP_k, \quad (4)$$

where  $K$  is the number of query images for each instance, and in this experiment,  $K = 10$ .

We also investigate the reasons for search failures. There are two possible types of search failures:

- 1) An object in the query image and its class are the same, but a different instance ID is retrieved.
- 2) A different object from the class of query image is retrieved.



TABLE II  
RESULTS OF ERROR ANALYSIS OF SEARCH RATES

Methods	Diff. instance ↓	Diff. class ↓
SimView (Ours)	<b>0.11</b>	<b>0.17</b>
SimSiam	0.17	0.19
DINOv2	0.25	0.20
SimCLR	0.18	0.19
✓CLIP [ResNet]	0.18	0.36
✓CLIP [ViT]	0.19	0.38

(Diff. instance) Different instances within the same class;  
(Diff. class) Object images with different classes.

We investigate the items of the two types of search failures in terms of the rate of failures using the assigned instance ID and object class labels from both the query image and the 3D semantic map. Each rate was calculated by performing the task 10 times, calculating the average number of failed searches in each environment, and then averaging these results across all environments.

#### D. Comparison Methods

We compare self-distillation methods, SimSiam [6] (with pre-trained ResNet50) and DINOv2 [7] (with pre-trained ViT), contrastive learning method with only image pairs, SimCLR [5] (with pre-trained ResNet50), and CLIP [2] (with pre-trained ResNet50 and ViT). In addition, we compare the pre-trained models and a fine-tuned model by SimView.

## VI. RESULT

### A. Comparison Unimodal Contrastive Learning and CLIP

Table I shows the average mAP over ten trials of similar image retrieval. SimSiam results in higher mAP values in many environments than other methods. In addition, SimCLR, another contrastive learning method other than SimSiam, results in higher mAP values in many environments. SimCLR is trained to maximize the similarity between two images generated through data augmentation and minimize the similarity with other images, which might lead to higher similarity between images of the same object. On the other hand, focusing on the results of CLIP, there tends to be a larger difference in mAP between SimSiam and CLIP than the difference in mAP between SimSiam and SimCLR. This is likely because CLIP, unlike unimodal contrastive learning, does not learn the similarity between different images of the same object. In addition, Tab. II illustrates the rate of classification failures. As shown in Tab. II, compared to ImageNet’s pre-trained SimSiam and SimView, CLIP retrieved images with a different instance or class from the query image at a higher rate. Furthermore, We show the three neighborhood images of the query image for each method in Fig. 6. By focusing on the bottom row in Fig. 6 where a TV image is given as the query, the neighborhood images retrieved by CLIP include the image from a different instance than the query image and the image different from the “TV”. On the other hand, all three images retrieved by SimSiam or SimCLR are the same instance as the query image. These observations suggest that pre-trained encoders with CLIP are

less adept at capturing fine visual similarities than Unimodal contrastive learning. Indeed, as shown in Fig. 7 (a), in the latent space of ImageNet’s pre-trained SimSiam, images of different instances belonging to the same class “TV” are separated in the latent space compared to the latent space of CLIP. Based on these results, we consider that the image encoder, which is pre-trained by the image contrastive task is effective for searching for an object identical to a query image in the environment.

### B. Comparison Pre-trained SimSiam and SimView

We also compare ImageNet’s [23] pre-trained SimSiam and SimSiam fine-tuned with images collected by exploring the environment. As shown in Tab. I, eight of the nine environments improved their metric scores, with scores on average about 8% better than pre-trained SimSiam. Furthermore, as shown in Fig. 7, images of the same instance are scattered in the latent space of ImageNet’s pre-trained SimSiam. Still, in the latent space of fine-tuned SimSiam on Env3, images of the same instance are densely distributed. Hence, compared to ImageNet’s pre-trained SimSiam, the fine-tuned SimSiam latent space can separate different instances from each other. We consider that this change in the distribution of images in the latent space led to the improvement of mAP. Indeed, as shown in the bottom row in Fig. 6, three neighborhood images retrieved SimSiam or SimCLR contain different instance images than the query image. On the other hand, three neighborhood images retrieved by fine-tuned SimSiam are the same as the query image.

## VII. CONCLUSION

We proposed a method, SimView, that leverages multi-view images based on a 3D semantic map of the environment and self-supervised learning by SimSiam to train an instance identification model on-site. This study investigated that an encoder trained through contrastive learning between images is effective for the task of a robot searching for the instance in environments that match the object in a given query image. The results showed that the encoder trained through self-distillation and SimView is effective for InstanceImageNav task compared to CLIP’s encoders pre-trained through contrastive learning between text and images, which are used in previous methods [3], [4].

A limitation of this validation is that both the observation and query images used in the validation are rendered images from 3D meshes containing RGB data, which may introduce domain shift effects with the training dataset of the encoder. In this validation, we assumed that the 3D map was pre-created. Therefore, in the future, it is necessary to combine the method of 3D semantic mapping [24], [25] and conduct validation in the real world.

### APPENDIX: VERIFICATION OF FINE-TUNING METHOD

We evaluate the effectiveness of fine-tuning a pre-trained SimSiam model by comparing two approaches: with an attached linear classifier or not. We also evaluate the performance difference between tuning all encoder layers versus tuning only a subset.



Fig. 6. Results of obtaining the top three-nearest neighbors in the latent space of the query image. Images with a red border indicate images that contain a different instance from the query image.

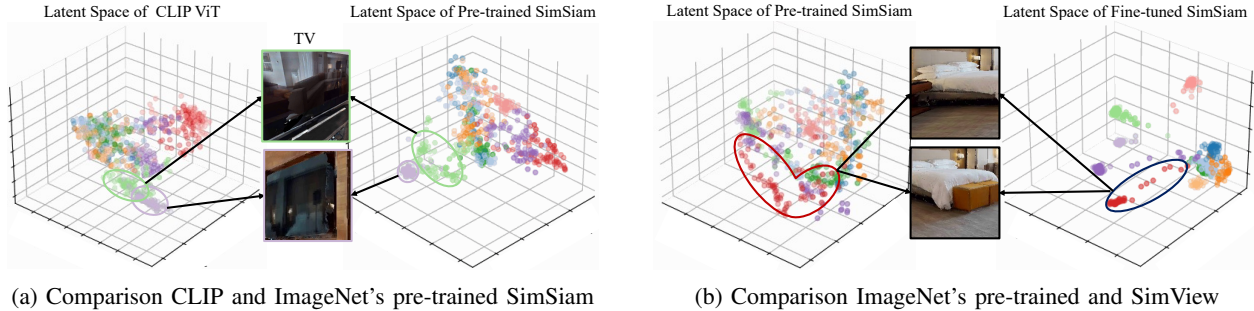


Fig. 7. Latent spaces of image encoders on Env. 3. In the scatter plot, different colors represent different instances. In (a), the latent space of SimSiam pre-trained on ImageNet more separated than the latent space of CLIP for images of different instances within the same class “TV”. In the red ellipse of (b), images of the same instance are scattered in the latent space of the pre-trained model. However, In the blue ellipse of (b), the latent space of SimView more closely clustered images of the same instance than the pre-trained model. In (a) and (b), the latent space of the pre-trained SimSiam is the same, but the perspective of the 3D scatter plot differs between the two figures.

### A. Multi-View Datasets

**Multi-view Images of Rotated Objects (MIRO)** [26]: MIRO includes images which only objects appear on a white background. This dataset has 12 object classes, with 10 instances of each class. Each instance was taken from 160 different camera poses. Therefore, the entire dataset contains 19,200 images. In this validation, half of the images in the dataset were used as the training and the rest as the testing. In addition, image labels are assigned per instance.

**Object Pose Invariance (ObjectPI)** [27]: This dataset differs from MIRO in that the images contain backgrounds other than the target object, similar to objects observed by the robot in its environment. In this dataset, image labels are assigned per instance. Each instance contains eight images taken from different directions. ObjectPI’s training data contains 400 different instances. In addition, the test data contains 100 types of instances. Therefore, in the verification using ObjectPI, we fine-tuned SimSiam using 3,200 images and tested using 800 images.

### B. Metrics

To evaluate the feature representation of the fine-tuned image encoder, we cluster the image feature representation obtained from the encoder using k-means and assign a cluster index to each image. Then, we use the Adjusted Rand Index (ARI) to quantify the degree of agreement between the true label assigned to each image in the dataset and the index assigned by k-means. A higher ARI score can be interpreted

TABLE III  
ARI SCORES IN EACH TRAINING CONDITION

Training Condition		MIRO		ObjectPI	
Update param.	Classifier	Train	Test	Train	Test
All	✓	0.49	0.53	0.14	0.20
Partial	✓	<b>0.85</b>	<b>0.59</b>	<b>0.50</b>	<b>0.66</b>
All	—	0.31	0.35	0.10	0.59
Partial	—	0.34	0.38	<u>0.48</u>	<u>0.59</u>
Pre-trained SimSiam		0.31	0.33	0.42	0.58

The training and test data were created using MIRO and ObjectPI.

as a feature representation that can discriminate between images of the same and different instances in the latent space.

### C. Training Condition

We fine-tuned ImageNet’s pre-trained SimSiam under four conditions: (a) updating all parameters with a classifier, (b) updating partial parameters with a classifier, (c) updating all parameters without a classifier, and (d) updating partial parameters without a classifier. Conditions (a) and (c) were run for 100 epochs, while conditions (b) and (d) were run for 50 epochs. The hyperparameters were kept consistent across all conditions except for the number of epochs. In conditions (b) and (d), parameters up to the third block of ResNet50 used in SimSiam are fixed, and the remaining parameters are updated (see Section IV-B for details).

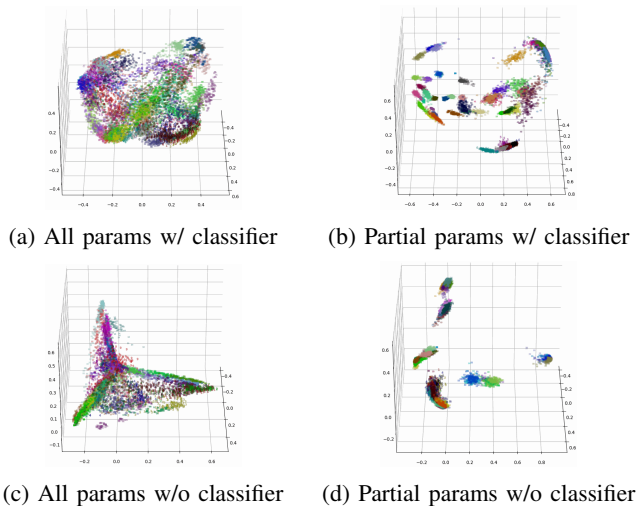


Fig. 8. Scatter plots that visualize the feature vectors calculated by image encoder trained with the MIRO dataset for each condition, reduced in dimension using PCA. Different colors represent different instances.

#### D. Result

Table III shows the ARI scores under each learning condition for the training data and test data created using MIRO and ObjectPI. From the Tab. III, it can be seen that the condition where some parameters were learned using a linear classifier had the highest ARI score for any dataset.

Fig. 8 shows the results of reducing the feature vectors of the images of the MIRO training dataset, which were calculated using the fine-tuned image encoder in each training condition, to three dimensions by principal component analysis (PCA). When training with a linear classifier, images are distributed throughout the latent space. Furthermore, when some parameters are updated with the attached classifier, images of different instances can be separated in the latent space of each instance compared to when all parameters are updated. Therefore, the ARI score is expected to be highest when a linear classifier was attached and only partial parameters were updated.

On the other hand, when fine-tuning is conducted using only contrastive learning, images distribute in only a part of the latent space, as shown in Fig. 8. This suggests that if fine-tuning is performed using only contrastive learning on a Multi-View Dataset, it is difficult to learn discriminative feature representation. This may be caused by the appearances of the same object in the Multi-View Dataset being different depending on the angle of view when the object is captured.

Based on these results, it is effective to fine-tune pre-trained SimSiam by adding a linear classifier to trained SimSiam in the fine-tuning module of the proposed system.

#### REFERENCES

[1] J. Krantz, S. Lee, *et al.*, “Instance-Specific Image Goal Navigation: Training Embodied Agents to Find Object Instances,” *arXiv preprint arXiv:2211.15876*, 2022.  
 [2] A. Radford, J. W. Kim, *et al.*, “Learning Transferable Visual Models from Natural Language Supervision,” in *PMLR International Conference on Machine Learning (ICML)*, 2021, pp. 8748–8763.

[3] B. Chen, F. Xia, *et al.*, “Open-Vocabulary Queryable Scene Representations for Real World Planning,” in *IEEE International Conference on Robotics and Automation (ICRA)*, 2023, pp. 11 509–11 522.  
 [4] N. M. M. Shafiullah, C. Paxton, *et al.*, “CLIP-Fields: Weakly Supervised Semantic Fields for Robotic Memory,” in *Robotics: Science and Systems (RSS)*, 2023.  
 [5] T. Chen, S. Kornblith, *et al.*, “A Simple Framework for Contrastive Learning of Visual Representations,” in *International Conference on Machine Learning (ICML)*, 2020, pp. 1597–1607.  
 [6] X. Chen and K. He, “Exploring Simple siamese Representation Learning,” in *IEEE/CVF Computer Vision and Pattern Recognition Conference (CVPR)*, 2021, pp. 15 750–15 758.  
 [7] M. Oquab, T. Darcet, *et al.*, “DINOv2: Learning Robust Visual Features without Supervision,” *arXiv preprint arXiv:2304.07193*, 2023.  
 [8] K. He, H. Fan, *et al.*, “Momentum Contrast for Unsupervised Visual Representation Learning,” in *IEEE/CVF Computer Vision and Pattern Recognition Conference (CVPR)*, 2020, pp. 9729–9738.  
 [9] T. Berg, J. Liu, *et al.*, “Birdsnap: Large-Scale Fine-Grained Visual Categorization of Birds,” in *IEEE/CVF Computer Vision and Pattern Recognition Conference (CVPR)*, 2014, pp. 2011–2018.  
 [10] S. Maji, E. Rahtu, *et al.*, “Fine-Grained Visual Classification of Aircraft,” *arXiv preprint arXiv:1306.5151*, 2013.  
 [11] M.-E. Nilsback and A. Zisserman, “Automated Flower Classification over a Large Number of Classes,” in *Indian Conference on Computer Vision, Graphics and Image Processing (ICGIP)*, 2008, pp. 722–729.  
 [12] M. Caron, H. Touvron, *et al.*, “Emerging Properties in Self-Supervised Vision Transformers,” in *IEEE/CVF International Conference on Computer Vision (ICCV)*, 2021, pp. 9650–9660.  
 [13] R. Balestriero, M. Ibrahim, *et al.*, “A Cookbook of Self-Supervised Learning,” *arXiv preprint arXiv:2304.12210*, 2023.  
 [14] I. Ben-Shaul, R. Shwartz-Ziv, *et al.*, “Reverse Engineering Self-Supervised Learning,” *Advances in Neural Information Processing Systems (NeurIPS)*, vol. 37, 2023.  
 [15] K. Yadav, R. Ramrakhya, *et al.*, “Offline Visual Representation Learning for Embodied Navigation,” in *Workshop on Reincarnating Reinforcement Learning at International Conference on Learning Representations (ICLR)*, 2023.  
 [16] T. Gervet, S. Chintala, *et al.*, “Navigating to Objects in the Real World,” *Science Robotics*, vol. 8, no. 79, p. eadf6991, 2023.  
 [17] K. He, X. Zhang, *et al.*, “Deep Residual Learning for Image Recognition,” in *IEEE/CVF Computer Vision and Pattern Recognition Conference (CVPR)*, 2016, pp. 770–778.  
 [18] T. Wang and P. Isola, “Understanding Contrastive Representation Learning through Alignment and Uniformity on the Hypersphere,” in *International Conference on Machine Learning (ICML)*, 2020, pp. 9929–9939.  
 [19] K. Yadav, R. Ramrakhya, *et al.*, “Habitat-Matterport 3D Semantics Dataset,” in *IEEE/CVF Computer Vision and Pattern Recognition Conference (CVPR)*, 2023, pp. 4927–4936.  
 [20] M. Savva, A. Kadian, *et al.*, “Habitat: A Platform for Embodied AI Research,” in *IEEE/CVF International Conference on Computer Vision (ICCV)*, 2019, pp. 9339–9347.  
 [21] I. Loshchilov and F. Hutter, “SGDR: Stochastic Gradient Descent with Warm Restarts,” in *International Conference on Learning Representations (ICLR)*, 2017.  
 [22] J. Philbin, O. Chum, *et al.*, “Object retrieval with large vocabularies and fast spatial matching,” in *IEEE/CVF Computer Vision and Pattern Recognition Conference (CVPR)*, 2007, pp. 1–8.  
 [23] J. Deng, W. Dong, *et al.*, “ImageNet: A Large-Scale Hierarchical Image Database,” in *IEEE/CVF Computer Vision and Pattern Recognition Conference (CVPR)*, 2009, pp. 248–255.  
 [24] M. Grinvald, F. Furrer, *et al.*, “Volumetric Instance-Aware Semantic Mapping and 3D Object Discovery,” in *IEEE Robotics and Automation Letters*, vol. 4, no. 3, 2019, pp. 3037–3044.  
 [25] A. Kanechika, L. El Hafi, *et al.*, “Interactive Learning System for 3D Semantic Segmentation with Autonomous Mobile Robots,” in *IEEE/SICE International Symposium on System Integration (SII)*, 2024.  
 [26] A. Kanezaki, Y. Matsushita, *et al.*, “RotationNet for Joint Object Categorization and Unsupervised Pose Estimation from Multi-View Images,” *IEEE Transactions on Pattern Analysis and Machine Intelligence*, vol. 43, no. 1, pp. 269–283, 2021.  
 [27] C.-H. Ho, P. Morgado, *et al.*, “PIEs: Pose Invariant Embeddings,” in *IEEE/CVF Computer Vision and Pattern Recognition Conference (CVPR)*, 2019, pp. 12 377–12 386.